Available online at www.sciencedirect.com

ScienceDirect

Procedia Engineering 88 (2014) 157 – 164

Procedia Engineering

www.elsevier.com/locate/procedia

International Symposium on Dynamic Response and Failure of Composite Materials, DRaF2014

Fracture mechanisms in epoxy composites reinforced with carbon nanotubes

S. Laurenzi[a]*, S. Botti[b], A. Rufoloni[c], M. G. Santonicola[d]

[a]*Department of Astronautic Electrical and Energy Engineering, Sapienza University of Rome, 00138 Rome, Italy*
[b]*ENEA, UTAPRAD-MNF, 00044 Frascati, Italy*
[c]*ENEA, UTFUS-COND, 00044 Frascati, Italy*
[d]*Department of Chemical Materials and Environmental Engineering, Sapienza University of Rome, 00161 Rome, Italy*

Abstract

Recent advances in nanotechnology and nanostructured materials offer the possibility to improve the mechanical properties of composite structures in terms of toughness and stiffness. In particular, in aerospace applications research efforts are focused on the design of advanced composite materials reinforced with carbon nanotubes (CNTs) that combine weight saving with multifunctional properties, including thermal, mechanical and electromagnetic ones. It is well known that carbon nanoparticles enhance the fracture strength, the modulus, and the yield strength of a polymer matrix through different mechanisms. However, despite the large amount of investigations on CNT-based composites and their relevant properties, there is a lack of understanding of the mechanisms leading to the failure of these materials under impact or static loads, which limits their use in practical applications. In this work, we present an experimental investigation of the fracture mechanisms of aerospace grade epoxy composites reinforced with multi-walled CNTs bridging the mechanical characterization with non-destructive methods, such as optical spectroscopy and electron microscopy. Our results show that it is possible to link the failure mechanisms of the nanostructured composite at the interface between the CNT and the epoxy matrix, namely cracking, pull-out and telescopic failure, with the molecular fingerprint of the carbon structure at the fracture surface after mechanical testing.

Peer-review under responsibility of the Organizing Committee of DRaF2014

Keywords: Composites, Fracture Mechanisms, Carbon Nanotubes, Aerospace Applications.

* Corresponding author. Tel.: +39 06 49919756; fax: +39 06 49919757.
E-mail address: susanna.laurenzi@uniroma1.it

Peer-review under responsibility of the Organizing Committee of DRaF2014
doi:10.1016/j.proeng.2014.11.139

1. Introduction

Epoxy matrices are widely used to fabricate composite structures with applications ranging from satellites to shipbuilding. The epoxy resins present a brittle behaviour due to the constrained plastic deformation that, combined with local stress concentration, may initiate cracks leading to an inadvertent failure.

Recent advances in nanotechnology and nanostructured materials offer the possibility to improve the mechanical properties of composite structures in terms of toughness and stiffness without significantly compromise other important properties. In the last decade, research efforts are focused on the design of advanced composite materials reinforced with carbon nanotubes (CNTs) that combine weight saving with multifunctional properties, including thermal, mechanical and electromagnetic ones [1]. It is well known that carbon nanoparticles enhance the fracture strength, the modulus, and the yield strength of a polymer matrix through different mechanisms [2-5]. However, despite the large amount of investigations on CNT-based composites and their relevant properties, there is a lack of understanding of the role of nanoparticles under impact or static loads, which limits their use in practical applications. In fact, the nanometer scale of the CNTs introduces a number of effects that act and interact, ultimately influencing the properties and the fracture mechanisms of the nano-reinforced composites in different ways with respect to the composites reinforced with macro-scale particles, such as graphite.

The morphological analysis of the fracture surfaces after mechanical testing can highlight the failure modes of the nano-reinforced composites and is a supporting analysis in the investigation of the fracture mechanisms, but gives few information on how far the nanoparticles have effectively participate to the carrying load, even in different form. In this context, Raman spectroscopy is a powerful tool for the characterization of carbon based materials, and is commonly used to investigate the exceptional electronic and phonon properties of carbon nanotubes [6]. Furthermore, Raman spectroscopy has been used to evaluate Young's modulus of single-walled and multi-walled carbon nanotubes embedded in epoxy film [7].

In this study, we investigate the possibility of detecting the failure modes of CNT-reinforced composites using Raman spectroscopy without the need of a fracture surface analysis by the laborious high-resolution scanning microscopy. We started the investigation from fracture surfaces of specimens subjected to tensile tests where the predominant failure modes of epoxy nanocomposites may be pull-out of CNTs and rupture of CNTs, which depend on the interfacial adhesion between of the outer tube of the MWCNTs and the epoxy matrix. For the same reason, we preferred the use of pristine MWCNTs instead of functionalized ones. In fact, covalent and non-covalent functionalization of carbon nanotubes is generally adopted to improve the dispersion procedure in the polymer matrix [8-9], but the CNTs surface modification affects their interfacial properties leading to a possible mix of failure modes [10]. Specimens for tensile tests were manufactured at 0, 0.5 and 1 wt% loading of MWCNTs dispersed in aerospace grade matrix, and the Young's modulus and the tensile strength of the materials were determined. High-resolution scanning electron microscopy (HR-SEM) images were collected at the fracture surfaces to correlate the Raman spectroscopy data with the failure modes of the epoxy nanocomposites. Raman analysis was performed also on both pristine MWCNTs powder and neat resin to highlight the contribution of MWCNTs to carry the tensile load.

2. Experimental

2.1. Materials

The carbon nanotubes used in this study were pristine MWCNTs produced by CVD from Nanocyl S.A. (Belgium). As given by the supplier, MWCNTs were 90% pure, with average outer diameter of 9.5 nm, an average length of 1.5 μm, and a surface area in the range of 250-300 m^2/g. The epoxy resin was the aerospace grade mono-component RTM6 manufactured by Hexcel (Hexcel Corp., USA).

2.2. Nanocomposites processing

MWCNT-reinforced epoxy specimens were prepared with 0.5 wt% and 1 wt% of nanotube loading. The most critical step during the sample preparation was the dispersion of the MWCNTs in the epoxy matrix so to obtain a homogeneous distribution. In fact, MWCNTs tend to form entanglements due to the van der Waals forces and the

high specific surface area. The dispersion procedure was tuned taking into account the temperature dependent viscosity, allowing both CNTs mobility into the matrix while preserving the resin pot life. The rheological behaviour of the RTM6 resin is strongly dependent on the temperature, passing from high value (1200 Pa·s) at room temperature to approximately 600 Pa·s at 80 °C. For this reason, the resin needed to be preheated before dispersion of the carbon nanoparticles. In this procedure, the resin was initially pre-heated up to 90 °C with a constant rate of 2 °C/min. This slow heating rate avoids stressing the material as a consequence of the temperature cycle. When the resin was homogenously heated, the desired amount of the MWCNTs was blended and mechanical mixed for about 20 min maintaining the temperature at about 90 °C. After that, the mixture was sonicated for 5 min with a sonication probe and then kept in an ultrasonic bath at 90 °C for about 90 min. In the latter step, the mixture was also degassed in order to eliminate the internal bubbles formed during the first 5 min of the sonication. The specimens were then prepared by pouring the mixture in a silicon mold and then cured at 160 °C for 2h. The free-standing specimens were further post-cured at 180 °C for 2h.

2.3. Test methods and analysis

Tensile tests were performed according to ASTM 638 standard, using an Instron machine with a load cell of 5KN, and using a dynamic extensometer to detect the tensile strain of the specimens. The morphology of the nanocomposites fracture surfaces after mechanical testing was investigated with a high-resolution scanning electron microscope (HR-SEM), using a Leo 1525 hot cathode field emission microscope with a resolution of 1.5 nm at 20kV.

Raman spectra were acquired with an integrated Raman system (i-Raman, B&W TEK Inc., USA), equipped with a video camera and a micro-positioning system for fine xyz adjustments and sample viewing. The excitation source was a diode laser emitting at 785 nm with a power scalable in the 3-300 mW range, focused through a 40X objective (laser beam diameter ~ 40 μm). The Raman spectra were measured in the wavelength range 789-1048 nm corresponding to Raman shifts of 75-3200 cm^{-1} (resolution 3 cm^{-1}). The MWCNTs were analyzed using the drop and dry technique. The nanotubes, in powder from, were diluted in distilled water (1 mg/mL), and a controlled volume drop was deposited on an aluminum substrate. The Raman spectra were acquired from the deposited film after water evaporation.

3. Results and discussion

Table 1 summarizes the results of the tensile tests for the neat resin (0 wt%) and the nanocomposites doped with different wt% of MWCNTs. Data are determined as an average of 5 tests per type of sample. Results show that the stiffness of the nanocomposites increases, whereas the tensile strength are slightly lower of the values of the neat resin. In particular, the Young's modulus increases of about 42% after adding 0.5 wt% MWCNTs, and of about 23% when adding 1 wt% MWCNTs. These results are consistent with the literature that identifies a threshold over which the mechanical properties decreases in the range 0.5-1 wt% of MWCNTs loading into a thermosetting polymer. This threshold is usually explained with the manufacturing limits of dispersing larger amounts of carbon nanoparticles into a thermosetting matrix because of their large specific surface and large aspect ratio. As a consequence, van der Waals forces create a mutual attraction of the CNTs, driving their aggregation into clusters inside the epoxy matrix even after disentanglement processes [9, 11].

Table 1. Tensile tests on neat epoxy and MWCNTs reinforced epoxy resin

MWCNTs contents (wt% vs. resin)	Tensile strength (*MPa*)	Young's modulus *(MPa)*
0	64 ± 5.7	2904 ± 122.7
0.5	57 ± 10.1	4115 ± 613.7
1	44.8 ± 8.6	3564.5 ± 780

HR-SEM images in Fig. 1 and Fig. 2 show the fracture surfaces of nanocomposites loaded with 1 wt% and 0.5 wt% of MWCNTs, respectively. As the images indicate, a good random distribution of the MWCNTs inside the epoxy matrix was achieved. Further, there is a remarkable fractographic difference between the well-known fracture surfaces of a neat epoxy resin, which exhibits a typical brittle behavior, and the fracture surfaces of the nanocomposites loaded with MWCNTs reported here. In the latter cases, the roughness of the surface is due to the deviation of the crack propagation that occurs when the crack meets a MWCNT or an agglomerate of them. The crack propagation is obstructed by the carbon nanoparticles incrementing the elastic modulus of the nanocomposites with respect to the neat resin.

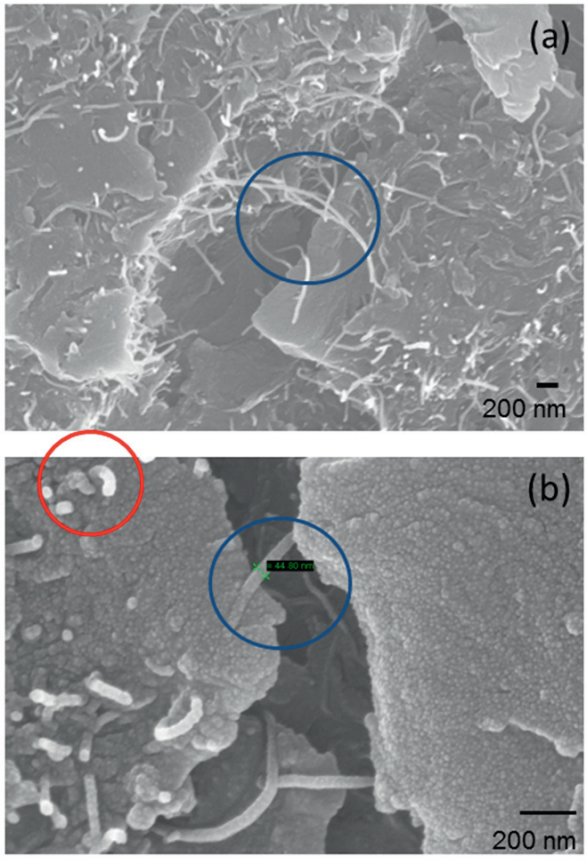

Fig. 1. HR-SEM images of the fracture surface of nanocomposite with 1 wt% loading of MWCNTs. Samples were coated with sputtered gold to improve the contrast, therefore the nanotube dimension appears bigger than the original size.

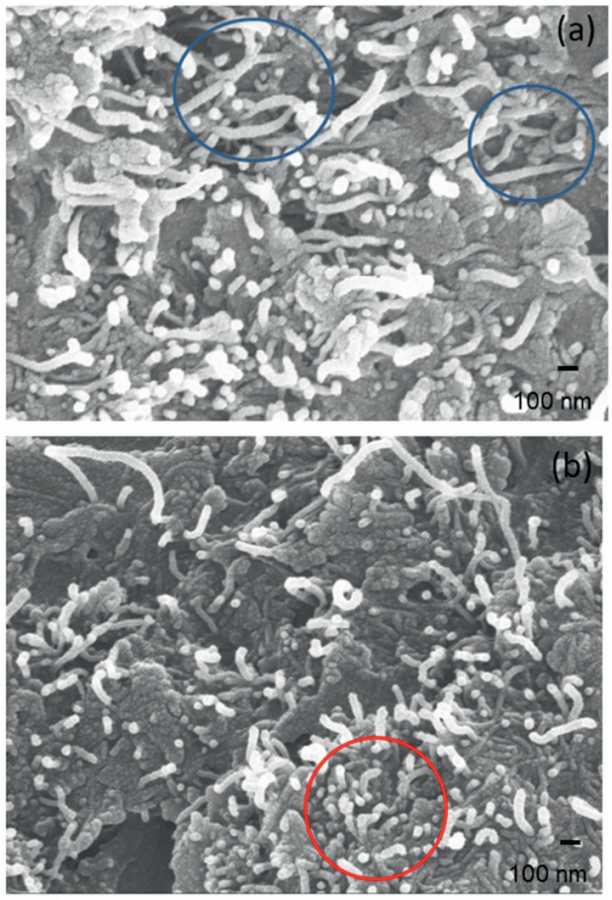

Fig. 2. HR-SEM images of the fracture surface of nanocomposite with 0.5 wt% loading of MWCNTs. Samples were coated with sputtered gold to improve the contrast, therefore the nanotube dimension appears bigger than the original size.

The Raman spectra of pure RTM6 (curve a) and pristine MWCNTs (curve b) that are incorporated in the epoxy matrix are reported in Fig. 3. The measured Raman lines of curve (a) can be attributed to the C–H out of plane deformation (796 and 893 cm^{-1}), the ring breathing (995 cm^{-1}), the SO_2 symmetric stretching (1190 cm^{-1}), the C–O stretch in epoxide (1270 cm^{-1}) and the C=C aromatic ring chain vibrations (1450 cm^{-1} and 1614 cm^{-1}, respectively). The Raman spectrum of the MWCNTs is dominated by two bands, which are characteristic of sp2 hybridized carbon: the D band (1310 cm^{-1}) which is a A1g symmetry breathing mode of sixfold graphitic rings and the G line (1606 cm^{-1}) corresponding to the in-plane bond stretching motion of carbon atoms pairs. The D mode is forbidden in perfect graphite and it becomes active due to the breaking of the wave-vector selection rule resulting from finite crystal size effects. It is also activated by the presence of in plane defects, grain boundary, substitutional hetero-atoms or other kind of defects which lower the dimension of crystalline perfect lattice [12-17].

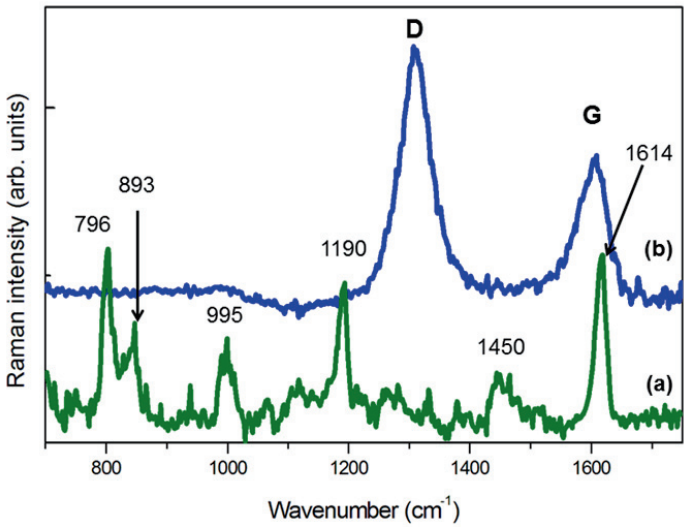

Fig. 3. Raman spectra of RTM6 (curve a) and MWNTs (curve b) excited at 785 nm.

Due to the inhomogeneity of the fracture surface, several random scans were performed, with the most reproducible results displayed in Fig. 4. In the curve a and b, the vibrational modes of MWCNTs and epoxy resin are overlapping at 1600 cm^{-1}, giving rise to a shoulder around 1590 cm^{-1} whose intensity increases with MWCNTs loading percentage in the composite. In some regions of the composite with 1 wt% of nanotubes, it was possible to record a Raman spectrum with only the D and G band of MWCNTs, without any contribution from the host matrix. The G band has a full width at half maximum (FWHM) of about 60 cm^{-1}, as that of pristine MWCNTs and a red-shifted peak at 1600 cm^{-1}. The shift of the G band peak toward lower/higher wavenumbers can be associated with the axial elongation/shortening of the C-C bond length in nanotube shell, under tensional loading and may be used to evaluate the strain percentage (ε_z) [5, 18-21] according to the following relation:

$$\frac{\Delta\omega}{\omega_0} = -\gamma(1-\nu_\tau)\varepsilon_z \tag{1}$$

where $\gamma = 1.24$ is the Gruneisen parameter and $\nu_\tau = 0.28$ is the Poisson ratio. The so obtained value of the strain percentage is 0.4 %, which translates in a tensile loading of incorporated MWCNTs. However, the relative shift depends on the direction of the nanotube axis and is maximal in the direction of the applied stress. Because the MWCNTs in the composites may have arbitrary direction, we measured an average shift of the G band peak.

The HR-SEM images at the fracture surfaces (Fig. 1-2) show that the nanotubes that are oriented orthogonally to the direction of the applied load exhibit a pull-out caused by the interfacial debonding (blue circles). In this case the resistance to the applied load is governed by the adhesion between the polymer molecules and the MWCNTs: the tensile stress is greater than the interaction forces between the outer layer of the MWCNTs and the epoxy polymer. On the other hand, MWCNTs that are oriented in the direction of the tensional loading appear broken at the break surface. This means that the a strong bonding occurs between the MWCNT and the host matrix that leads to a complete rupture of the nanotube or to a fracture of the outer layer and a telescopic pull-out of the inner tubes, in agreement with the observed red shifting of MWCNTs G band in the Raman spectroscopy after mechanical tests. However, the corresponding ε_z is smaller than 1, and therefore, following literature data [16-20], the strain behaviour should be still that of elastic response.

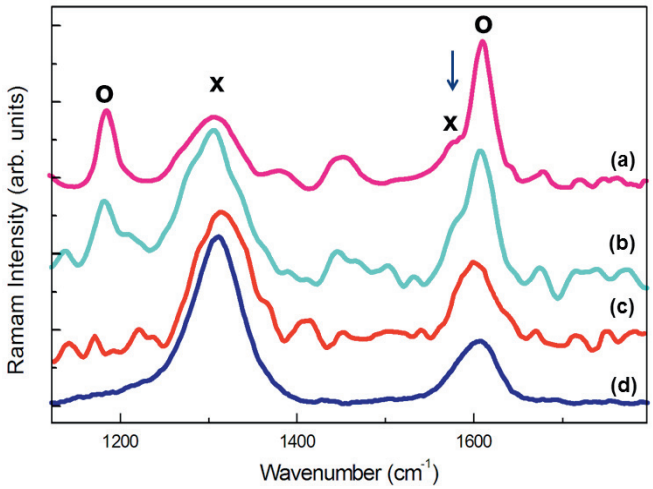

Fig. 4. Raman spectra of MWNTs/RTM6 composite fracture surfaces. Curve a: MWCNTs percentage in epoxy resin: 0.5wt%. Curve b: MWCNTs percentage in epoxy resin: 1.0 wt%. Curve c: MWCNTs percentage in epoxy resin: 1 wt% (different sample region). Curve d: Raman spectrum of pristine MWCNTs reported for clarity. Legend: o, RTM6; x, MWCNTs.

This apparent contradiction can be reconciled by taking into account that most likely only the outermost layer of the nanotube is loaded due to the interfacial bonding. Because of the relatively weak bonding between layers, then the load is not transferred allowing slipping between the tube walls, decreasing the measured shift that is averaged over the whole nanotube. Moreover, as discussed before, we have also to take into account that the tube with the axis orthogonal to the stress direction, as those in the blue circles in Fig. 2a, do not contribute to the red shift. This hypothesis is supported by the HR-SEM images reported in Fig. 2, in which the nanotubes pulled out from the matrix are kinked with knots (see the red circles in Fig. 2b).

4. Conclusions

In this work, we show that Raman spectroscopy can be successfully used to characterize the tensile deformation of a MWCNTs/epoxy composite. Well-defined Raman spectra were obtained at the surface of the fractures, and from the observed Raman band shifts, the stress transfer from the polymer matrix to the MWCNTs could be deduced. All the experimental measurements are consistent with the model of nanotube fracture due to the strong interfacial bonding of the outer nanotube layer with the host resin matrix.

References

[1] R.F. Gibson, A review of recent research on mechanics of multifunctional composite materials and structures, Compos. Struct. 92 (2010) 2793-2810.
[2] S. Laurenzi, R. Pastore, G. Giannini, M. Marchetti, Experimental study of impact resistance in multi-walled carbon nanotube reinforced epoxy, Compos. Struct. 99 (2013) 62-68.
[3] S.S. Wicks, R.G. de Villoria, B.L. Wardle, Interlaminar and intralaminar reinforcement of composite laminates with aligned carbon nanotubes, Compos. Sci. Technol. 70 (2010) 20-28.
[4] V. Kostopoulos, A. Baltopoulos, P. Karapappas, A. Vavouliotis, A. Paipetis, Impact and after-impact properties of carbon fibre reinforced composites enhanced with multi-wall carbon nanotubes, Compos. Sci. Technol. 70 (2010) 553-563.
[5] C.S. Grimmer, C.K.H. Dharan, Enhancement of delamination fatigue resistance in carbon nanotube reinforced glass fiber/polymer composites, Compos. Sci. Technol. 70 (2010) 901-908.
[6] M.S. Dresselhaus, G. Dresselhaus, R. Saito, A. Jorio, Raman spectroscopy of carbon nanotubes, Physics Reports 409 (2005) 47-99.
[7] O. Lourie, H.D. Wagner, Evaluation of Young's modulus of carbon nanotubes by micro-Raman spectroscopy, J. Mater. Res. 13 (1998) 2418-2422.
[8] S. Laurenzi, M. Sirilli, M. Pinna, M.G. Santonicola, DNA-Assisted Dispersion of Multi-Walled CNTs in Epoxy Polymer Matrix, Materials Research Society Symposium Proceedings 1700 (2014).
[9] P.-C. Ma, N.A. Siddiqui, G. Marom, J.-K. Kim, Dispersion and functionalization of carbon nanotubes for polymer-based nanocomposites: A

review, Composites, Part A 41 (2010) 1345-1367.
[10] F.H. Gojny, M.H.G. Wichmann, B. Fiedler, K. Schulte, Influence of different carbon nanotubes on the mechanical properties of epoxy matrix composites – A comparative study, Compos. Sci. Technol. 65 (2005) 2300-2313.
[11] L. Vaisman, H.D. Wagner, G. Marom, The role of surfactants in dispersion of carbon nanotubes, Adv. Colloid Interface Sci. 128–130 (2006) 37-46.
[12] S. Botti, R. Ciardi, M.L. Terranova, S. Piccirillo, V. Sessa, M. Rossi, M. Vittori-Antisari, Self-assembled carbon nanotubes grown without catalyst from nanosized carbon particles adsorbed on silicon, Appl. Phys. Lett. 80 (2002) 1441-1443.
[13] P.C. Eklund, J.M. Holden, R.A. Jishi, Vibrational modes of carbon nanotubes; Spectroscopy and theory, Carbon 33 (1995) 959-972.
[14] H. Jantoljak, J.P. Salvetat, L. Forró, C. Thomsen, Low-energy Raman-active phonons of multiwalled carbon nanotubes, Appl. Phys. A 67 (1998) 113-116.
[15] A. Jorio, M.A. Pimenta, A.G.S. Filho, R. Saito, G. Dresselhaus, M.S. Dresselhaus, Characterizing carbon nanotube samples with resonance Raman scattering, New J. Phys. 5 (2003) 139.
[16] A.M. Rao, E. Richter, S. Bandow, B. Chase, P.C. Eklund, K.A. Williams, S. Fang, K.R. Subbaswamy, M. Menon, A. Thess, R.E. Smalley, G. Dresselhaus, M.S. Dresselhaus, Diameter-Selective Raman Scattering from Vibrational Modes in Carbon Nanotubes, Science 275 (1997) 187-191.
[17] R. Saito, G. Dresselhaus, M.S. Dresselhaus, Electronic structure of double‐layer graphene tubules, J. Appl. Phys. 73 (1993) 494-500.
[18] R. Andrews, M.C. Weisenberger, Carbon nanotube polymer composites, Curr. Opin. Solid State Mater. Sci. 8 (2004) 31-37.
[19] C.A. Cooper, R.J. Young, M. Halsall, Investigation into the deformation of carbon nanotubes and their composites through the use of Raman spectroscopy, Composites, Part A 32 (2001) 401-411.
[20] M.N. Iliev, A.P. Litvinchuk, S. Arepalli, P. Nikolaev, C.D. Scott, Fine structure of the low-frequency Raman phonon bands of single-wall carbon nanotubes, Chem. Phys. Lett. 316 (2000) 217-221.
[21] D. Puglia, L. Valentini, I. Armentano, J.M. Kenny, Effects of single-walled carbon nanotube incorporation on the cure reaction of epoxy resin and its detection by Raman spectroscopy, Diamond Relat. Mater. 12 (2003) 827-832.